Mississippi State University
Scholars Junction

Theses and Dissertations | Theses and Dissertations

5-7-2016

Evaluation of Thiol Raman Activities and pKa Values using Internally Referenced Raman-based pH Titration

Nuwanthi Savindrika Suwandaratne

Follow this and additional works at: https://scholarsjunction.msstate.edu/td

Recommended Citation

Suwandaratne, Nuwanthi Savindrika, "Evaluation of Thiol Raman Activities and pKa Values using Internally Referenced Raman-based pH Titration" (2016). *Theses and Dissertations*. 2078.
https://scholarsjunction.msstate.edu/td/2078

This Graduate Thesis - Open Access is brought to you for free and open access by the Theses and Dissertations at Scholars Junction. It has been accepted for inclusion in Theses and Dissertations by an authorized administrator of Scholars Junction. For more information, please contact scholcomm@msstate.libanswers.com.

Evaluation of thiol Raman activities and pKa values using internally referenced Raman-based pH titration

By

Nuwanthi Suwandaratne

A Thesis
Submitted to the Faculty of
Mississippi State University
in Partial Fulfillment of the Requirements
for the Degree of Master of Science
in Chemistry
in the Department of Chemistry

Mississippi State, Mississippi

May 2016

Copyright by

Nuwanthi Suwandaratne

2016

Evaluation of thiol Raman activities and pKa values using internally referenced Raman-based pH titration

By

Nuwanthi Suwandaratne

Approved:

_____

Dongmao Zhang
(Major Professor)

_____

David O. Wipf
(Committee Member)

_____

Todd E. Mlsna
(Committee Member)

_____

Stephen C. Foster
(Graduate Coordinator)

_____

Rick Travis
Interim Dean
College of Arts & Sciences

Name:Nuwanthi Suwandaratne

Date of Degree: May 7, 2016

Institution: Mississippi State University

Major Field: Chemistry

Major Professor: Dongmao Zhang

Title of Study: Evaluation of thiol Raman activities and pKa values using internally referenced Raman-based pH titration

Pages in Study: 45

Candidate for Degree of Master of Science

Thiols are one of the most important classes of chemicals used broadly in organic synthesis, biological chemistry, and nanosciences. Thiol pK_a values are key indicators of thiol reactivity and functionality. This study is an internally-referenced Raman-based pH titration method that enables reliable quantification of thiol pK_a values for both mono- and di-thiols in water. The degree of thiol ionization is monitored directly using the peak intensity of the S-H stretching feature relative to an internal reference peak as a function of solution pH. The thiol pK_a values and Raman activity relative to its internal reference were then determined by curve-fitting the experimental data with equations derived on the basis of the Henderson-Hasselbalch equation. Using this Raman titration method, first and second thiol pK_a values for 1,2-benzenedithol in water were determined for the first time. This method is convenient to implement and its underlying theory is easy to follow.

DEDICATION

I would like to dedicate this body of work to my mother Thamara Suwandaratne, father Kithsiri Suwandaratne, brother Asela Suwandaratne, and my husband Harsha Madushanka for their love and enormous support.

ACKNOWLEDGEMENTS

First and foremost I would like to thank my research advisor Dr. Dongmao Zhang who has supported me throughout my Master's career. I am grateful for the knowledge he has instilled in me. I would also like to express my gratitude to the members of my graduate committee, Dr. David O. Wipf and Dr. Todd E. Mlsna, for their advice and guidance.

I express my sincere gratitude to Dr Juan Hu (DePaul University) for his assistance on statistical analysis of data. I also like to thank my lab mates: Manuel Gadogbe, Charles Nettles, Ganganath Perera, Kumudu Siriwardana, Sumudu Athukorale, Sandamini Alahakoon who have been friendly, open-minded, and supportive friends.

My most heartfelt acknowledgment goes to my family who have given me support in times of doubt, particularly my mother for her unconditional love and faith shown me throughout my life, and my husband whose constant encouragement and belief helped me complete this research study successfully.

Lastly, I would like to extend my thanks to the big family of the Chemistry Department at Mississippi State University.

TABLE OF CONTENTS

LIST OF TABLES

LIST OF FIGURES

LIST OF ABBREVIATIONS AND CHEMICALS

K_a	Acid dissociation constant
ITC	Isothermal Titration Calorimetry
NMR	Nuclear Magnetic Resonance
AuNPs	Gold nanoparticles
NA	Not available
Cys	Cysteine
GSH	Glutathione
2-ME	2-Mercaptoethanol
CyA	Cysteamine
3-MPS	Sodium 3-mercapto-1-propanesulfonate
DTT	Dithiothreitol
1,4-BDT	1,4-Benzenedithiol
1,2-BDT	1,2-Benzenedithiol
DMSO	Dimethyl sulfoxide

CHAPTER I

INTRODUCTION

(This project has been published in *Anal. Chem*. 2016,

DOI :10.1021/acs.analchem.5b04241)

1.1 Acid dissociation constant (K_a)

The K_a is a quantitative indication of the strength of an acid in solution. It is the equilibrium constant for a weak acid (*HA*) in equilibrium with its conjugate base (A^-) in aqueous solution (1.1).[1]

$$HA(aq) + H_2O(l) \rightleftharpoons A^-(aq) + H_3O^+(aq) \quad (1.1)$$

Therefore the K_a is;

$$K_a = \frac{[A^-] \times [H_3O^+]}{[HA]} \quad (1.2)$$

The K_a can also be expressed as the logarithm of its reciprocal, called the pK_a.

$$pK_a = -\log K_a \quad (1.3)$$

Thus, the weaker the acid, the larger the pK_a value is.

1.1.1 pH titration

The experimental determination of pK_a values is usually performed using titrations. A theoretical titration curve for a monoprotic acid is shown below in Figure 1.1.

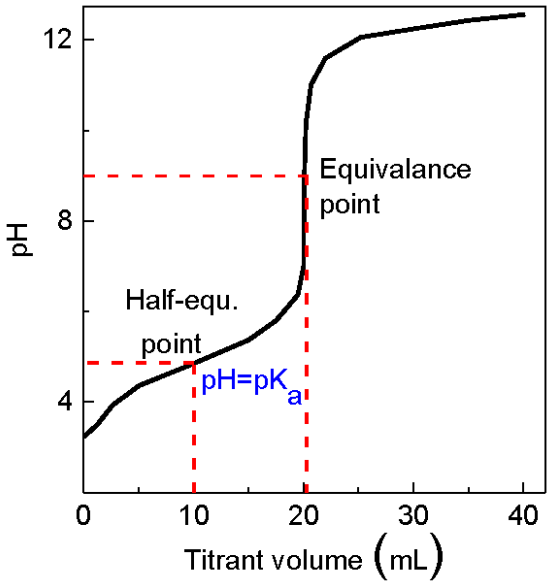

Figure 1.1 The titration curve of a weak monoprotic acid.

The titration curve is a plot of pH against the titrant volume. The relatively flat portion of the titration curve extending about 1 pH unit on either side of its half equivalence point is called the buffer region. In this zone, the titrant has much less effect on pH than outside the buffer range. At the half-equivalence point in the titration, exactly half of the HA initially present will have been neutralized, thus making the *HA* and A^- concentrations equal. Therefore, the K_a of a weak acid is equal to the hydronium ion concentration at the half-equivalence point, which can be used to determine pK_a.[1-2]

1.2 Introduction to thiols

The thiol (RS-H) functional group is ubiquitous, existing in many organic and bio-molecules. Compared to oxygen and hydrogen, the electronegativity difference between sulfur and hydrogen is smaller, thus making the polarity of the S-H bond smaller than that of the hydroxyl group. Thiols have a higher acidity relative to the corresponding

alcohol[3] (thiophenol has a pK_a of 6.5[4] versus 10 for phenol[5] and ethanethiol has a pK_a of 10.6[6] versus 16 for ethanol[7]). Therefore, thiols can be treated with alkali metal hydroxides to obtain thiolates as shown in equation 1.4.

$$RS-H \xrightarrow[-H_2O]{NaOH} RS^{-}Na^{+} \qquad (1.4)$$

Organothiols and thiolated synthetic- and bio-polymers have been used extensively in metallic nanoparticle applications including surface enhanced Raman spectroscopy, molecular electronics, and biosensing.[8-13] Biological thiols like glutathione and cysteine have multiple functions in vital biological processes in humans, animals and plants.[14-17]

One key indicator of thiol reactivity is its pK_a value. Generally, there are several methods available for pK_a determination.[18] Existing methods for thiol pK_a determination include potentiometry, UV-vis, NMR, and ITC.[19-25]

1.3 Raman spectroscopy

In 1928, the Indian physicist C.V. Raman discovered the Raman phenomenon for the first time. For this discovery, he was awarded the 1931 Nobel Prize in Physics. Raman spectroscopy is a form of vibrational spectroscopy which arises due to changes in the polarizability of molecules.[26-27]

1.3.1 Theory of Raman spectroscopy

In Raman spectroscopy, molecules are excited using monochromatic light, a laser source, to a virtual state, which is not quantized. When the excited molecules return to the ground electronic state through light scattering, the frequency of the scattered photon is

shifted in relative to the excitation frequency. Those frequency shifts are characteristic of the probed molecules. This inelastic light scattering is called the Raman effect.[26-27]

1.3.2 Wave model of Raman and Rayleigh scattering

The electric field (E) of a beam of radiation having a frequency v_0 can be described by the following equation;

$$E = E_0 \cos(2\pi v_0 t) \tag{1.5}$$

Where, E_0 is the amplitude of the wave and t is time. Once the electric field of the radiation interacts with the electron cloud of the analyte, an induced dipole moment (P) forms,

$$P = \alpha E \tag{1.6}$$

Here, α is the polarizability of the bond, which varies with bond length as follows;

$$\alpha = \alpha_0 + (r - r_{eq})(\frac{\partial \alpha}{\partial r}) \tag{1.7}$$

Where, α_0 is the polarizability of the bond at the equilibrium internuclear separation (r_{eq}) and r is the internuclear separation at any instant. Internuclear separation is related to the frequency of molecular vibrations (v_v) as follows;

$$(r - r_{eq}) = r_m \cos(2\pi v_v t) \tag{1.8}$$

Where, r_m is the maximum internuclear separation. Therefore,

$$\alpha = \alpha_0 + (\frac{\partial \alpha}{\partial r}) r_m \cos(2\pi v_v t) \tag{1.9}$$

Thus, the induced dipole moment can be written as,[27]

$$P = \alpha_0 E_0 \cos(2\pi\nu_0 t) + \frac{E_0}{2} r_m \left(\frac{\partial\alpha}{\partial r}\right) \cos[2\pi(\nu_0 - \nu_v)t] + \frac{E_0}{2} r_m \left(\frac{\partial\alpha}{\partial r}\right) \cos[2\pi(\nu_0 + \nu_v)t] \quad (1.10)$$

Depending on the frequency difference between the scattered and incident light, there are three types of emitted radiation: Rayleigh, Stokes, and anti-Stokes scattering (Figure 1.2) which corresponds to the first, second and third terms in the equation 1.10. Rayleigh scattering is elastic scattering, because the scattered radiation has the same frequency as the excitation laser. The scattered radiation with lower frequency than the incident radiation ($\nu_0 - \nu_v$) is known as Stokes scattering, and radiation with higher frequency than the incident radiation ($\nu_0 + \nu_v$) is called anti-Stokes scattering. Due to the fact that the majority of molecules will be found in the ground state at room temperature, usually Raman measurements are performed based on Stokes scattering.[26-27]

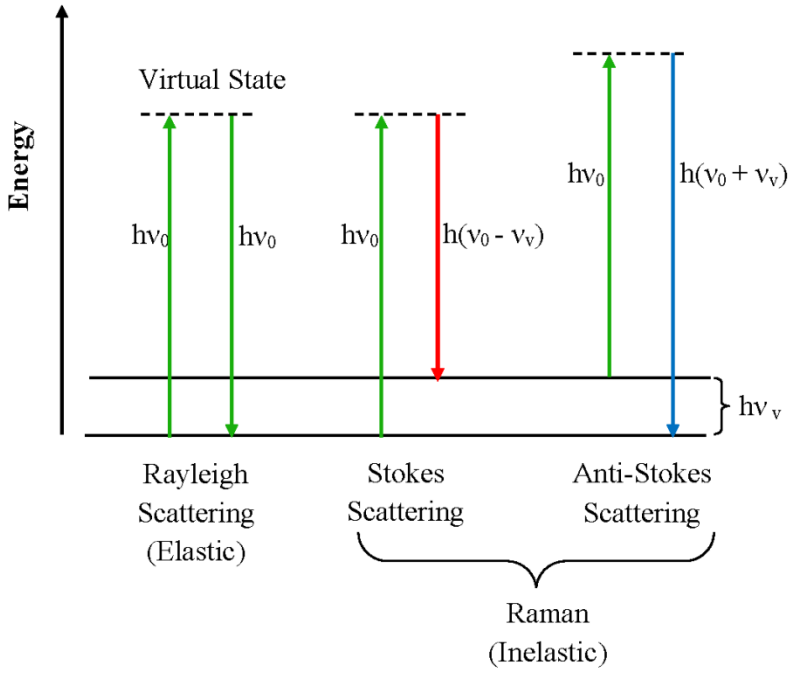

Figure 1.2 Energy level diagram of the states involved in Raman signals.

1.3.3 Internal reference in Raman spectroscopy

The Raman signal intensities are affected not only by the amount of sample, but also by instrument and sampling parameters including sample dilutions, excitation laser power, Raman photon collection efficiency and the laser spectral integration times. The effect of such variations can be eliminated by use of an internal reference.[28]

The internal reference in Raman spectroscopy is a Raman peak from the analyte molecule itself, or a Raman peak from an exogenous chemical that has a relatively intense and well-defined Raman feature. The key criteria for choosing the internal reference is that it can be readily identified and quantified.[29] The Raman cross section of the internal reference used for thiol pK_a and Raman activity determination should be insensitive to the solution pH. These criteria ensure that the peak intensity ratio between the S-H stretch and the internal reference peak differs when S-H is ionized.

1.4 Theoretical consideration

1.4.1 Determination of pK_a of monothiol

This internally-referenced Raman titration method for determination of monothiol pK_a can be mathematically justified using the standard Henderson-Hasselbalch equation (1.11) in combination with equations 1.12 and 1.13. The latter two equations define the peak intensity ratios of the S-H stretching feature versus its internal reference peak for non-ionized thiols and partially ionized thiols at specified pH, respectively.

$$pH = pK_a + \log \frac{[RS^-]_{pH}}{[RS-H]_{pH}} \tag{1.11}$$

$$R^0 = \frac{I^0_{SH}}{I^0_{ref}} = \frac{[RS-H]_0 \sigma_{S-H} K}{[REF]_0 \sigma_{ref} K} = \frac{[RS-H]_0 \sigma_{S-H}}{[REF]_0 \sigma_{ref}} \tag{1.12}$$

$$R^{pH} = \frac{I_{SH}^{pH}}{I_{ref}^{pH}} = \frac{[RS-H]_{pH}\,\sigma_{S-H}\,K_{pH}}{[REF]_0\,\sigma_{ref}\,K_{pH}} = \frac{[RS-H]_{pH}\,\sigma_{S-H}}{[REF]_0\,\sigma_{ref}} \tag{1.13}$$

$$pH = pK_a + \log\frac{R^0 - R^{pH}}{R^{pH}} \tag{1.14}$$

I_{SH}^{0} and I_{ref}^{0} are the S-H stretching and internal reference peak intensities under the conditions that all thiol groups remain non-ionized. I_{SH}^{pH} and I_{ref}^{pH} are the S-H stretching and internal reference peak intensities of the partially ionized thiol at a specified pH. *K* and K_{pH} are instrument and sampling parameters that affect the signal intensity as a function of the analyte concentration. These parameters include sample dilutions induced by the titrants, excitation laser power, Raman photon collection efficiency, and the laser spectral integration times. $[RS-H]_{pH}$ and $[RS^{-}]_{pH}$ are the concentrations of the non-ionized and thiolated thiols, respectively, at specified pH conditions. $[RS-H]_0$ and $[REF]_0$ are the concentrations of the thiol and internal reference, respectively, under conditions that all thiol groups remain non-ionized. Importantly, $[RS-H]_0$ and $[REF]_0$ can be identical if a different Raman feature from the same thiol molecule is used as the internal reference. σ_{SH} and σ_{ref} are the Raman cross-sections of the thiol stretching mode and its internal reference feature peak, respectively.

Eq. 1.14 implies that the thiol pK_a is equal to the solution pH at which the intensity ratio of S-H stretching versus its internal reference is exactly half of that when all thiols are non-ionized. In this case, $R^{pH} = R^0/2$. However, pinpointing the "half point" is challenging. This is because R^0 can only be approximated by the peak intensity

ratio of S-H versus the internal reference in solutions for which the pH is significantly lower than the thiol pK_a value. However, obtaining high quality Raman spectra with non-ionized thiols can be challenging because non-ionized thiols usually have lower solubility than ionized ones. Furthermore, locating the exact "half point" is statistically impossible in realistic experimental measurements. This is due to the difficulty of controlling the degree of thiol ionization induced by each titration. Eq. 1.14 can be rearranged into Eq. 1.15 (derivation is shown in Results and Discussions) in which the pK_a and R^0 values can be directly obtained by fitting the experimental data of R^{pH} as a function of solution pH using the standard Boltzmann function. No experimental R^0 is needed and all the titration data are utilized for determining the thiol pK_a values.

This curve-fitting can be performed using commercial software such as Origin Pro by choosing the Boltzmann function (Eq. 1.16) as the fitting function and presetting the values of *d* and A_2 in Eq. 1.10 as 1/2.303 and 0, respectively. This data fitting procedure can be termed as constraint Boltzmann function fitting because *d* and A_2 are preset to those values to ensure Eq. 1.16 is identical to Eq. 1.15. A simulated Raman-based pH titration curve derived according to Eq.1.15 was shown in Figure 1.3. Apparently, one can readily pinpoint the monothiol pK_a values graphically by monitoring thiol Raman intensity over a wide pH range. However, in practice, this visual examination method can be problematic because of the measurement errors. In contrast, the least-squares curve fitting method is much more robust because it gives the most likely statistical thiol pK_a value that best explains all the titration data.

$$R^{pH} = \frac{R^0}{1 + e^{2.303(pH - pK_a)}} \tag{1.15}$$

$$y = \frac{A_1 - A_2}{1 + e^{(x - x_0)/d}} + A_2 \tag{1.16}$$

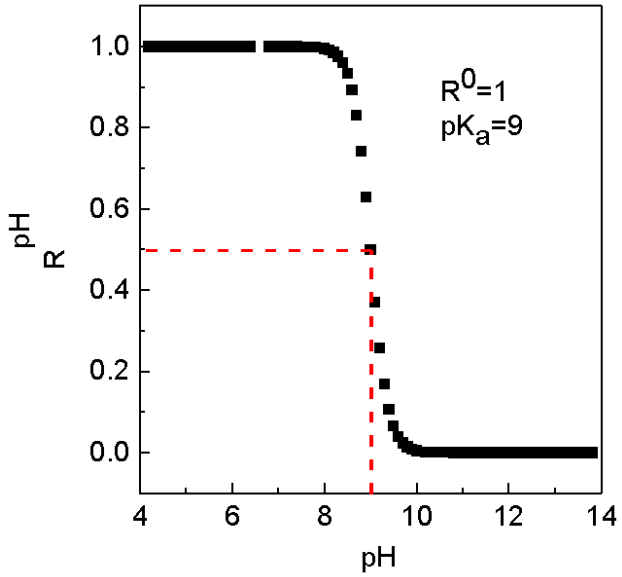

Figure 1.3 Simulated Raman-based pH titration curve plotted using Eq. 1.15.

1.4.2 Determination of thiol Raman activity

While the pK_a value reflects the acidity of the thiol group, one can derive the thiol Raman cross-section from R^0. Indeed, rearranging Eq. 1.12 leads to Eq. 1.17 and further to Eq. 1.18 and Eq. 1.19 in which [*thiol*] represents the total concentration of non-ionized and ionized thiols. The reason Eq. 1.17 is equivalent to Eq. 1.18 or Eq. 1.19 is that titration and thiol ionization does not change the concentration ratio of the internal reference and the total thiols, regardless of whether the thiols are totally non-ionized, partially or completely ionized. As a result, one can simply use the thiol and internal reference sample concentration in the initial titration solution for the thiol Raman activity calculation. Eq. 1.18 or Eq. 1.19 indicates that after obtaining R^0 from the curve-fitting,

one can readily determine the thiol relative Raman cross-section defined as the Raman cross-section ratio of the thiol and the internal reference peak.

$$\frac{\sigma_{S-H}}{\sigma_{ref}} = R^0 \frac{[REF]_0}{[RS-H]_0} \tag{1.17}$$

$$\frac{\sigma_{S-H}}{\sigma_{ref}} = R^0 \frac{[REF]_{pH}}{[thiol]_{pH}} \tag{1.18}$$

$$\frac{\sigma_{S-H}}{\sigma_{ref}} = R^0 \frac{[REF]_{ini}}{[thiol]_{ini}} \tag{1.19}$$

1.4.3 Determination of pK_a of dithiol

The above theoretical consideration is for monothiol (one S-H group) pK_a. For molecules that contain multiple thiols, the pK_a value for individual thiols can also be resolved by using this internally-referenced Raman titration method. For simplicity, only the functional forms for curve-fitting determination of the first and second pK_a for molecules that contain two thiols are shown. Detailed derivation of Eq. 1.20 is shown in Results and Discussions.

$$R^{pH} = \frac{R^0 + \alpha R^0 10^{(pH-pK_{a1})}}{1+10^{(pH-pK_{a1})}(1+10^{(pH-pK_{a2})})} \tag{1.20}$$

Here α is the ratio of the S-H Raman cross-section of the monothiolated versus non-ionized dithiols. This value is 0.5 as deprotonation of the first thiol has no effect on the Raman cross-section of the remaining thiol in the dithiol. R^0 and R^{pH} are the peak intensity ratios of the S-H stretching feature versus its internal reference peak for non-ionized dithiol and partially ionized dithiol at specified pH, respectively. pK_{a1} and pK_{a2} are the first and second acid dissociation constants of the dithiol, respectively. The only

experimental parameter needed for curve-fitting determination of the first and second thiol pK_a values, together with α and R^0, are the R^{pH} values as a function of solution pH. A computer program for curve-fitting determination of these parameters was developed using R program (Appendix A), a computer software package commonly used in statistical data analysis.

Importantly, pK_{a1} and pK_{a2} values can be approximated graphically or by fitting the experimental data in different pH regions using the standard Boltzmann function but with different constraints (Figure 1.4). When solution pH is significantly smaller than pK_{a2} but covers the region in which the first thiol ionizes, Eq. 1.20 can be simplified into Eq. 1.21, which is equivalent to Eq. 1.22. The latter is equivalent to the standard Boltzmann function (Eq. 1.16) in which A_1 is R^0 for the curve-fitting and the ratio between A_2/A_1 is α.

$$R^{pH} = \frac{R^0 + \alpha R^0 10^{(pH - pK_{a_1})}}{1 + 10^{(pH - pK_{a_1})}} \tag{1.21}$$

$$R^{pH} = \frac{R^0 - \alpha R^0}{1 + e^{2.303(pH - pK_{a_1})}} + \alpha R^0 \tag{1.22}$$

If the solution pH is equal to pK_{a1}, and is significantly smaller than pK_{a2}, Eq.1.21 is simplified into Eq. 1.23.

$$R^{pK_{a_1}} = \frac{R^0 + \alpha R^0}{2} \tag{1.23}$$

When the solution pH is significantly larger than pK_{a1} and covers the region in which the second thiol ionizes, Eq. 1.20 can be further simplified into Eq. 1.24; this is again a constrained Boltzmann function.

$$R^{pH} = \frac{\alpha R^0}{1 + e^{2.303(pH - pK_{a_2})}} \tag{1.24}$$

Under conditions in which the solution pH is equal to pK_{a2} but significantly larger than pK_{a1}, Eq. 1.24 can be further simplified into Eq. 1.25.

$$R^{pK_{a2}} = \frac{\alpha R^0}{2} \tag{1.25}$$

Figure 1.4 shows the series of simulated Raman based pH titration curves in which pK_{a1}, R^0, and α were kept to be 6.0, 1.0, and 0.5, respectively, but the value of pK_{a2} changes from 7, 8, 9, 10, and 11, respectively. Evidently, one can estimate the pK_{a1} and pK_{a2} values graphically if both thiols can be ionized and their pK_a differs by 3 pK_a units or more.

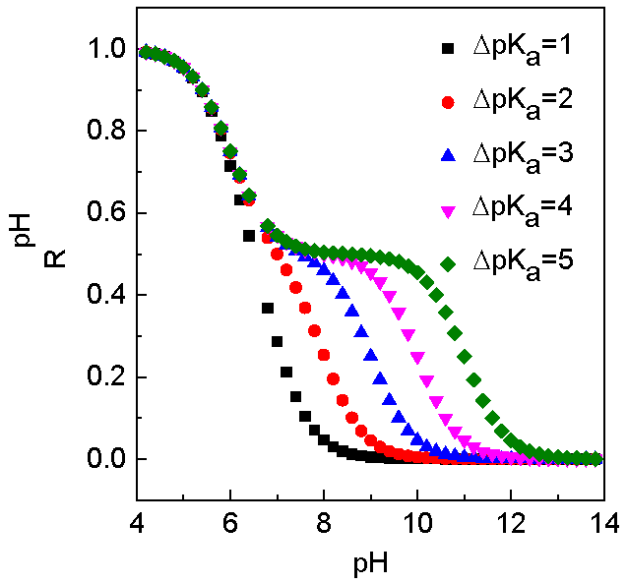

Figure 1.4 Simulated Raman-based pH titration curve plotted using Eq. 1.20. ΔpK_a is the difference between pK_{a2} and pK_{a1}. ΔpK_a was changed from 1 to5. (pK_{a1}= 6, R^0 = 1 and α = 0.5).

Once R^0 and α are known, the S-H Raman cross-section in the non-ionized ($\sigma_{S\text{-}H}^{intact}$) and monothiolated ($\sigma_{S\text{-}H}^{mono}$) dithiols can be calculated using Eq. 1.26, and Eq. 1.27.

$$\sigma_{S\text{-}H}^{intact} = R^0 \frac{[REF]_{ini}\sigma_{ref}}{[\mathrm{d}ithiol]_{ini}} \tag{1.26}$$

$$\sigma_{S\text{-}H}^{mono} = \alpha\sigma_{S\text{-}H}^{intact} \tag{1.27}$$

CHAPTER II

MATERIAL AND METHODS

2.1 Chemicals and equipment

Dithiothreitol and sodium 3-mercapto-1-propanesulfonate were purchased from Fluka and 1,4-benzenedithiol from Alfa Aesar. All other chemicals were purchased from Sigma-Aldrich. Nanopure water (18.2 MΩ-cm) was used throughout the experiments. Normal Raman spectra were obtained with a Horiba LabRam HR 800 confocal Raman microscope system and a 633 nm Raman excitation laser with 13 mW laser power. The acquisition time for Cys, GSH, 3-MPS, and 2-ME is 20 s, and 50 s for CyA and the dithiols. The spectra shown in the figures are an average of 10 individual spectra. The RamChip slides used for Raman spectral acquisition were obtained from Z&S Tech. LLC. The solution pH was measured using a calibrated AB 15, Accumet pH electrode. Origin Pro was used as the software for curve fitting and R program was developed in this work for dithiol pK_a determination using equation 1.20 (Appendix A).

2.2 Raman titrations of soluble thiols

Known amounts or saturation quantities of water-soluble thiols were dissolved in 2 mL aliquots of 150 mM Na_2SO_4 solution. Excess thiol in each solution was removed through membrane filtration using a pore size of 0.2 μm in diameter. Each thiol solution was titrated with a 500 mM NaOH solution using a 10 μL pipette. The solution mixture

was vortexed after each NaOH addition, followed with pH measurement and Raman acquisition.

2.3 Raman titrations of thiols with poor water solubility

Both 1,2-BDT and 1,4-BDT are poorly soluble in water in their non-ionized forms. However, their solubility in basic solution increases significantly. 1,4-BDT was first added into 2 mL of 1 M NaOH followed with filtration removal of undissolved thiol. The saturated thiol-containing solution was then titrated using 1 M HCl solution. As 1,2-benzendithiol is a liquid, 20 μL was dissolved in 2 mL of 1 M NaOH and then titrated using 1 M HCl solution. Solutions were vortexed after each HCl addition, followed with pH measurement and Raman acquisition.

CHAPTER III

RESULTS AND DISCUSSIONS

3.1 Drawbacks of existing methods for thiol pK_a determination

The reliable evaluation of thiol pK_a is challenging due to several reasons. Thiol pK_a determination methods are essentially all indirect techniques and are often susceptible to interference. For example, pinpointing thiol pK_a in multifunctional thiol-containing molecules through potentiometric pH titration is almost impossible in many cases. This is because of the interference from other ionizable functional groups such as amines and carboxyl groups.[30] The UV-vis method monitors the UV-vis spectral change as a function of solution pH. It requires the thiol-containing molecule to contain a chromophore that is sensitive only to the thiol's ionization.[24,31] This imposes a significant constraint on the general application of this method. Indeed, it has been recently demonstrated that the pK_a values of 1,4-benzenedithiol (1,4-BDT) determined with the UV-vis method are highly erroneous.[32] Only one 1,4-BDT thiol can be deprotonated even in highly concentrated (2 M) NaOH solution. This is in contrast to the first and second pK_a values of 6 and 7.7 reported on the basis of UV-vis titration of 1,4-BDT.[33] The more recent ITC method deduces the thiol pK_a value on the basis of the kinetics of thioether formation reactions as a function of the solution pH. A relatively large number of control and sample measurements must be carefully conducted in order

to get the reaction rate constants at each of the pH values. Consequently, this technique involves laborious sample preparations, measurements, and intensive data analysis.[21]

About two decades ago, Thomas et al. proposed a Raman-based method for determining thiol pK_a values by monitoring the S-H intensity in a series of thiol-containing solutions that have the same concentration but different pHs.[34] The thiol pK_a value corresponds to the solution pH at which the S-H stretching intensity is exactly half of that for the non-ionized thiol. This Raman-based method enables direct visualization of the degree of thiol ionization. This is because the peak position of the S-H feature is around ~2600 cm^{-1}, well-separated from other Raman peaks in Raman spectra obtained with essentially any samples. However, the experimental procedure of this original Raman method is cumbersome. It employs nitrogen in air as the external reference for correcting S-H peak intensity variations induced by measurement conditions. Although this external reference enables correction of S-H peak intensity variations induced by the fluctuation in laser excitation power and detection sensitivities, it is unable to compensate for signal variation induced by changes in photon excitation and collection efficiencies and in sample concentrations. Therefore, care must be taken to ensure the Raman sampling geometries to be exactly the same for different samples.

Instead of using nitrogen in air as the external reference, this study employed internal references for determining the peak intensity ratio of the S-H peak relative to its internal reference peak. Since the internal reference can compensate for S-H signal variation induced by sample dilution, this method enables the use of Raman-based pH titration to determine the thiol pK_a.

3.2 Detailed derivation of equation for monothiol pK_a determination

$$pH - pK_a = \log \frac{R^0 - R^{pH}}{R^{pH}} \tag{3.1}$$

$$10^{(pH-pK_a)} = \frac{R^0 - R^{pH}}{R^{pH}} \tag{3.2}$$

By simplifying 3.2,

$$10^{(pH-pK_a)} = \frac{R^0}{R^{pH}} - 1 \tag{3.3}$$

By rearranging 3.3,

$$R^{pH} = \frac{R^0}{1+10^{(pH-pK_a)}} \tag{3.4}$$

$$R^{pH} = \frac{R^0}{1+e^{2.303(pH-pK_a)}} \tag{3.5}$$

3.3 Detailed derivation of equation for dithiol pK_a determination

$$pH = pK_{a1} + \log \frac{[RS_2H^-]_{pH}}{[RS_2H_2]_{pH}} \tag{3.6}$$

$$pH = pK_{a2} + \log \frac{[RS_2{}^{2-}]_{pH}}{[RS_2H^-]_{pH}} \tag{3.7}$$

By adding 3.6 and 3.7,

$$2pH = pK_{a1} + pK_{a2} + \log \frac{[RS_2{}^{2-}]_{pH}}{[RS_2H_2]_{pH}} \tag{3.8}$$

At specified pH, the concentration of intact dithiol $[RS_2H_2]_0$ is the sum of the concentration of non-ionized dithiol at that pH $[RS_2H_2]_{pH}$ and the concentrations of monothiolated dithiol $[RS_2H^-]_{pH}$ and completely deprotonated dithiol $[RS_2{}^{2-}]_{pH}$.

$$[RS_2H_2]_0 = [RS_2H_2]_{pH} + [RS_2H^-]_{pH} + [RS_2{}^{2-}]_{pH} \tag{3.9}$$

By rearranging 3.9,

$$[RS_2{}^{2-}]_{pH} = [RS_2H_2]_0 - [RS_2H_2]_{pH} - [RS_2H^-]_{pH} \tag{3.10}$$

By substituting $[RS_2{}^{2-}]_{pH}$ in 3.8,

$$2pH = pK + \log \frac{[RS_2H_2]_0 - [RS_2H_2]_{pH} - [RS_2H^-]_{pH}}{[RS_2H_2]_{pH}} \tag{3.11}$$

Where,

$$pK = pK_{a1} + pK_{a2} \tag{3.12}$$

$$R^0 = \frac{\mathrm{I}^0_{\mathrm{SH}}}{\mathrm{I}^0_{\mathrm{ref}}} = \frac{[RS_2H_2]_0 \sigma_{S_2H_2}}{[REF]_0 \sigma_{ref}} \tag{3.13}$$

By rearranging,

$$[RS_2H_2]_0 = \frac{[REF]_0 \ \sigma_{ref}}{\sigma_{S_2H_2}} R^0 \tag{3.14}$$

By rearranging 3.6,

$$[RS_2H^-]_{pH} = [RS_2H_2]_{pH}.10^{pH-pK_{a1}} \tag{3.15}$$

$$R^{pH} = \frac{I^{pH}_{SH}}{I^{pH}_{ref}} = \frac{[RS_2H_2]_{pH} \sigma_{S_2H_2} + [RS_2H^-]_{pH} \sigma_{S_2H^-}}{[REF]_0 \ \sigma_{ref}} \tag{3.16}$$

By substituting $[RS_2H^-]_{pH}$ (3.15) in 3.16,

$$R^{pH} = \frac{[RS_2H_2]_{pH}\,\sigma_{S_2H_2} + ([RS_2H_2]_{pH}.10^{pH-pK_{a1}})\,\sigma_{S_2H^-}}{[REF]_0\,\sigma_{ref}} \tag{3.17}$$

By rearranging 3.17,

$$[RS_2H_2]_{pH} = \frac{[REF]_0\sigma_{ref}}{\sigma_{S_2H_2} + \sigma_{S_2H^-} \times 10^{pH-pK_{a1}}} R^{pH} \tag{3.18}$$

By substituting $[RS_2H_2]_0$ (3.14) and $[RS_2H^-]_{pH}$ (3.15) in 3.11,

$$2pH = pK + \log \frac{\frac{[REF]_0\sigma_{ref}}{\sigma_{S_2H_2}} R^0 - [RS_2H_2]_{pH} - [RS_2H_2]_{pH}.10^{pH-pK_{a1}}}{[RS_2H_2]_{pH}} \tag{3.19}$$

By simplifying,

$$2pH = pK + \log \frac{\frac{[REF]_0\sigma_{ref}}{\sigma_{S2H2}} R^0 - [RS_2H_2]_{pH}(1+10^{pH-pK_{a1}})}{[RS_2H_2]_{pH}} \tag{3.20}$$

Substituting $[RS_2H_2]_{pH}$ (3.18) in 3.20,

$$2pH = pK + \log \frac{\frac{[REF]_0\sigma_{ref}}{\sigma_{S_2H_2}} R^0 - \frac{[REF]_0\sigma_{ref}}{\sigma_{S_2H_2} + \sigma_{S_2H^-} \times 10^{pH-pK_{a1}}} R^{pH}(1+10^{pH-pK_{a1}})}{\frac{[REF]_0\sigma_{ref}}{\sigma_{S_2H_2} + \sigma_{S_2H^-} \times 10^{pH-pK_{a1}}} R^{pH}} \tag{3.21}$$

By multiplying both numerator and denominator of log term by $\frac{\sigma_{S_2H_2}}{[REF]_0\sigma_{ref}}$,

$$(2pH = pK + \log \frac{[\frac{[REF]_0 \sigma_{ref}}{\sigma_{S_2H_2}} R^0 - \frac{[REF]_0 \sigma_{ref}}{\sigma_{S_2H_2} + \sigma_{S_2H^-} \times 10^{pH-pK_{a1}}} R^{pH}(1+10^{pH-pK_{a1}})] \frac{\sigma_{S_2H_2}}{[REF]_0 \sigma_{ref}}}{[\frac{[REF]_0 \sigma_{ref}}{\sigma_{S_2H_2} + \sigma_{S_2H^-} \times 10^{pH-pK_{a1}}} R^{pH}] \frac{\sigma_{S_2H_2}}{[REF]_0 \sigma_{ref}}})$$

(3.22)

By simplifying,

$$2pH = pK + \log \frac{R^0 - \frac{\sigma_{S_2H_2} R^{pH}(1+10^{pH-pK_{a1}})}{\sigma_{S_2H_2} + \sigma_{S_2H^-} \times 10^{pH-pK_{a1}}}}{\frac{\sigma_{S_2H_2}}{\sigma_{S_2H_2} + \sigma_{S_2H^-} \times 10^{pH-pK_{a1}}} R^{pH}}$$

(3.23)

By simplifying,

$$2pH = pK + \log \frac{R^0 - \frac{R^{pH}(1+10^{pH-pK_{a1}})}{1+(\sigma_{S_2H^-}/\sigma_{S_2H_2})10^{pH-pK_{a1}}}}{\frac{R^{pH}}{1+(\sigma_{S_2H^-}/\sigma_{S_2H_2}).10^{pH-pK_{a1}}}}$$

(3.24)

But,

$$\sigma_{S_2H^-} / \sigma_{S_2H_2} = \alpha$$

(3.25)

$$2pH = pK + \log \frac{R^0 - \frac{R^{pH}(1+10^{pH-pK_{a1}})}{1+\alpha.10^{pH-pK_{a1}}}}{\frac{R^{pH}}{1+\alpha.10^{pH-pK_{a1}}}}$$

(3.26)

By multiplying both numerator and denominator of log term by $1+\alpha.10^{pH-pK_{a1}}$,

$$2pH = pK + \log \frac{R^0(1+\alpha 10^{pH-pK_{a1}}) - R^{pH}(1+10^{pH-pK_{a1}})}{R^{pH}}$$

(3.27)

$$2pH = pK + \log \frac{R^0 + R^0 \alpha 10^{pH-pK_{a1}} - R^{pH} - R^{pH} 10^{pH-pK_{a1}}}{R^{pH}} \tag{3.28}$$

By rearranging 3.28,

$$10^{(2pH-pK)} = \frac{R^0 + \alpha R^0 10^{(pH-pK_{a_1})}}{R^{pH}} - (1 + 10^{(pH-pK_{a1})}) \tag{3.29}$$

$$R^{pH} = \frac{R^0 + \alpha R^0 10^{(pH-pK_{a_1})}}{10^{(2pH-pK)} + (1 + 10^{(pH-pK_{a1})})} \tag{3.30}$$

$$R^{pH} = \frac{R^0 + \alpha R^0 10^{(pH-pK_{a_1})}}{10^{(2pH-pK_{a1}-pK_{a2})} + (1 + 10^{(pH-pK_{a1})})} \tag{3.31}$$

By simplifying 3.31,

$$R^{pH} = \frac{R^0 + \alpha R^0 10^{(pH-pK_{a_1})}}{1 + 10^{(pH-pK_{a1})}(1 + 10^{(pH-pK_{a2})})} \tag{3.32}$$

3.4 Thiol pK_a of monothiols

The model monothiols (Figure 3.1) used in this work include cysteine (Cys), glutathione (GSH), 2-mercaptoethanol (2-ME), cysteamine (CyA) and sodium 3-mercapto-1-propanesufonate (3-MPS).

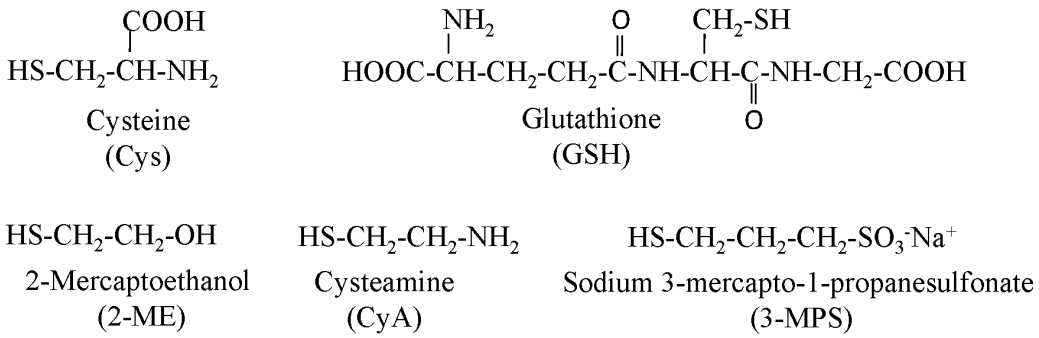

Figure 3.1 Structures of the model monothiols

Figures 3.2 to 3.6 show the data of model monothiols Cys, GSH, 2-ME, CyA, and 3-MPS in which Na_2SO_4 was added as the exogenous internal reference. Evidently, it is challenging to estimate the thiol pK_a value for these organothiols on the basis of their pH titration curves (pH value as a function of the volume of the titrant, Figure B of Figure 3.2 to 3.6). In contrast, one can readily determine the pK_a value by Boltzmann function curve-fitting the Raman titration data for the intensity ratio of the S-H stretching peak versus its internal reference as a function of solution pH (Figure C of Figure 3.2 to 3.6).

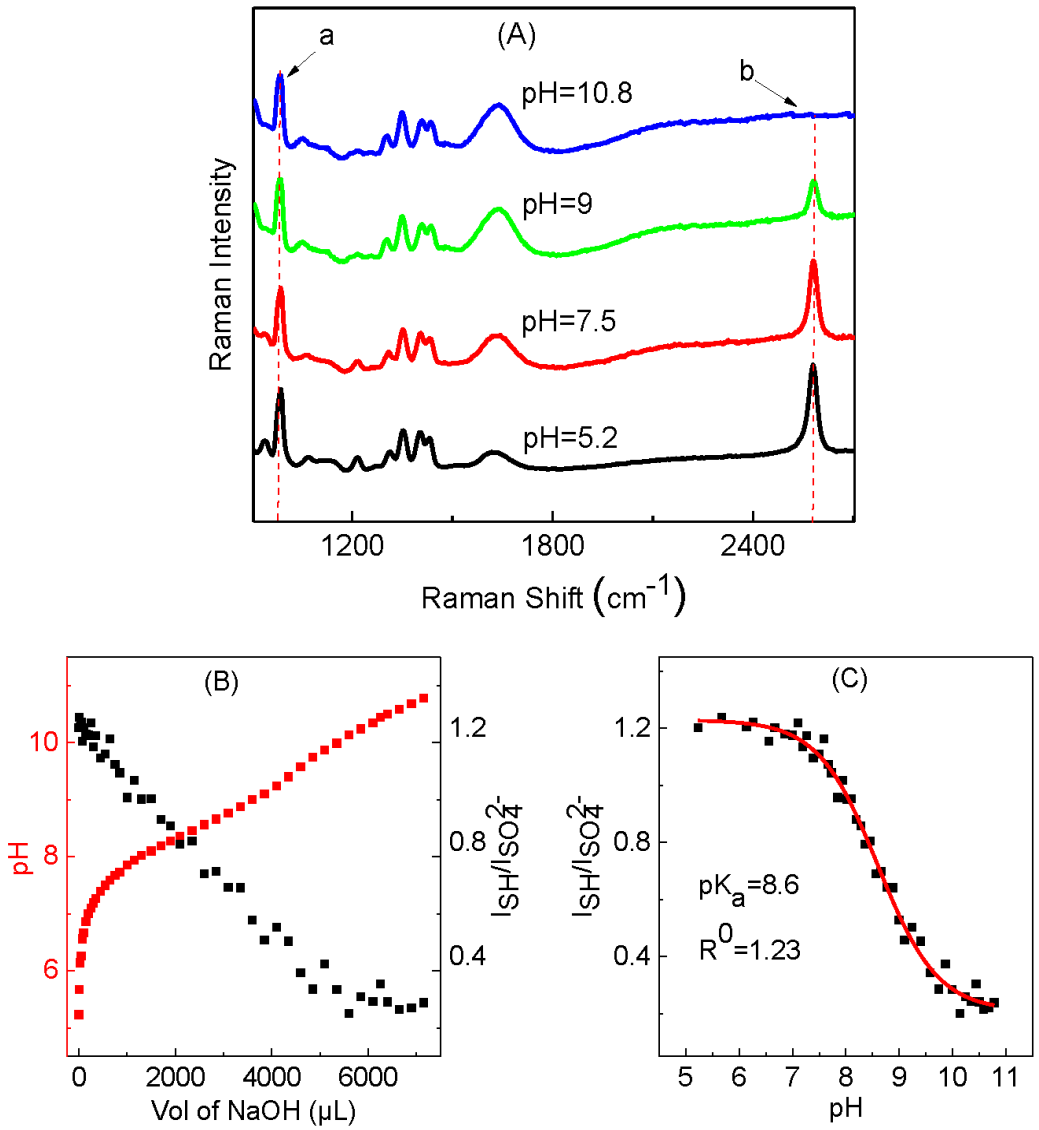

Figure 3.2 Raman-based pH titration for pK_a determination of the thiol group in Cys

(A) Representative Raman spectra of Cys as a function of solution pH. ((a) SO_4^{2-}, (b) S-H peak). The spectra are normalized by the sulfate peak intensity. (B) Solution pH (red) and relative S-H peak intensity (black) as a function of titrant (500 mM NaOH) volume. (C) The relative S-H peak intensity as a function of solution pH. The solid curve and the data shown in (C) are the Boltzmann function curve-fitting output of the experimental data using Origin Pro. The Cys and Na_2SO_4 concentrations in the initial solutions are 0.83 M and 0.15 M, respectively.

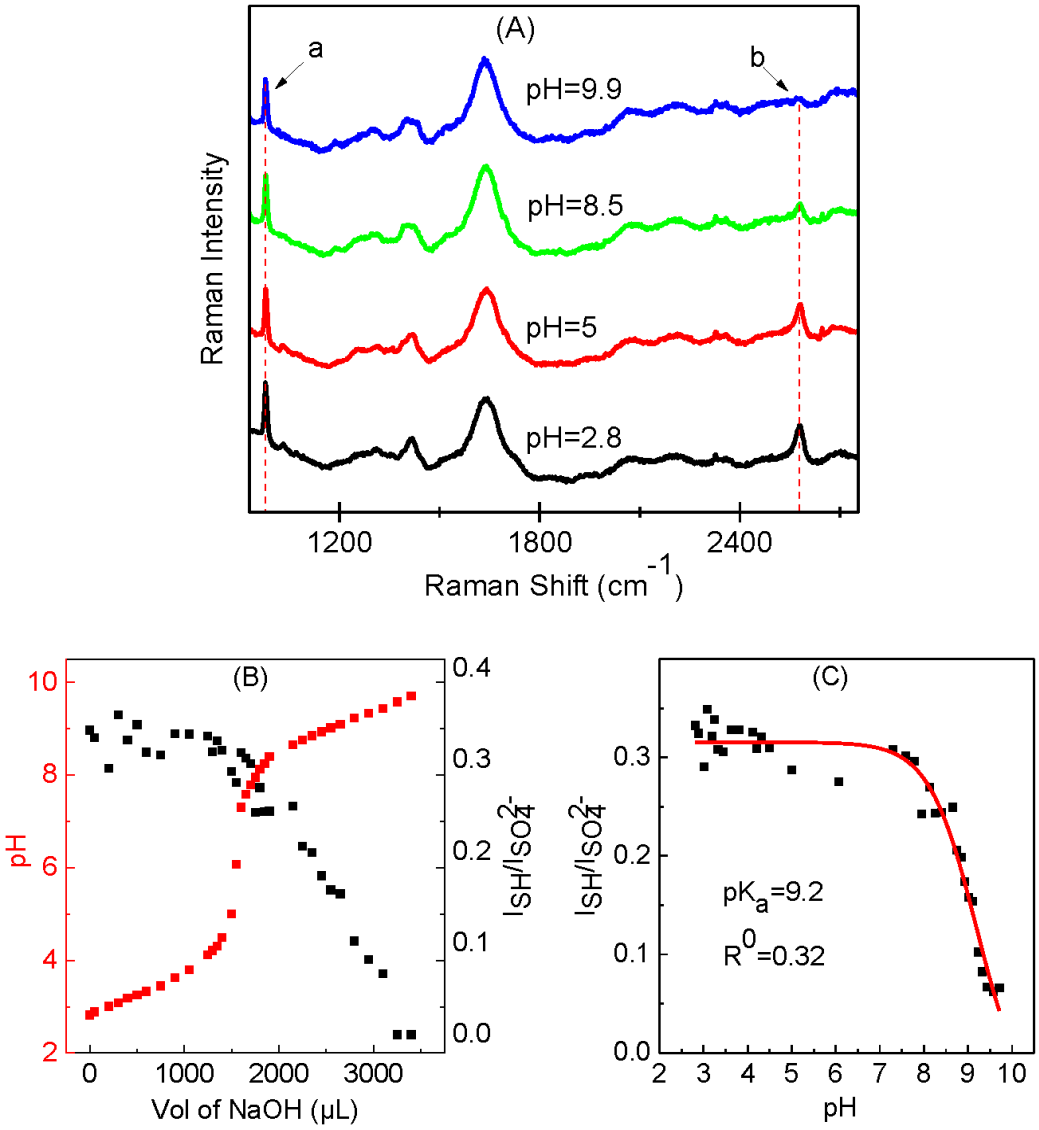

Figure 3.3 Raman-based pH titration for pK_a determination of the thiol group in GSH

(A) Representative Raman spectra of GSH as a function of solution pH. ((a) SO_4^{2-}, (b) S-H peak). The spectra are normalized by the sulfate peak intensity. (B) Solution pH (red) and relative S-H peak intensity (black) as a function of titrant (500 mM NaOH) volume. (C) The relative S-H peak intensity as a function of solution pH. The solid curve and the data shown in (C) are the Boltzmann function curve-fitting output of the experimental data using Origin Pro. The GSH and Na_2SO_4 concentrations in the initial solutions are 0.22 M and 0.15 M, respectively.

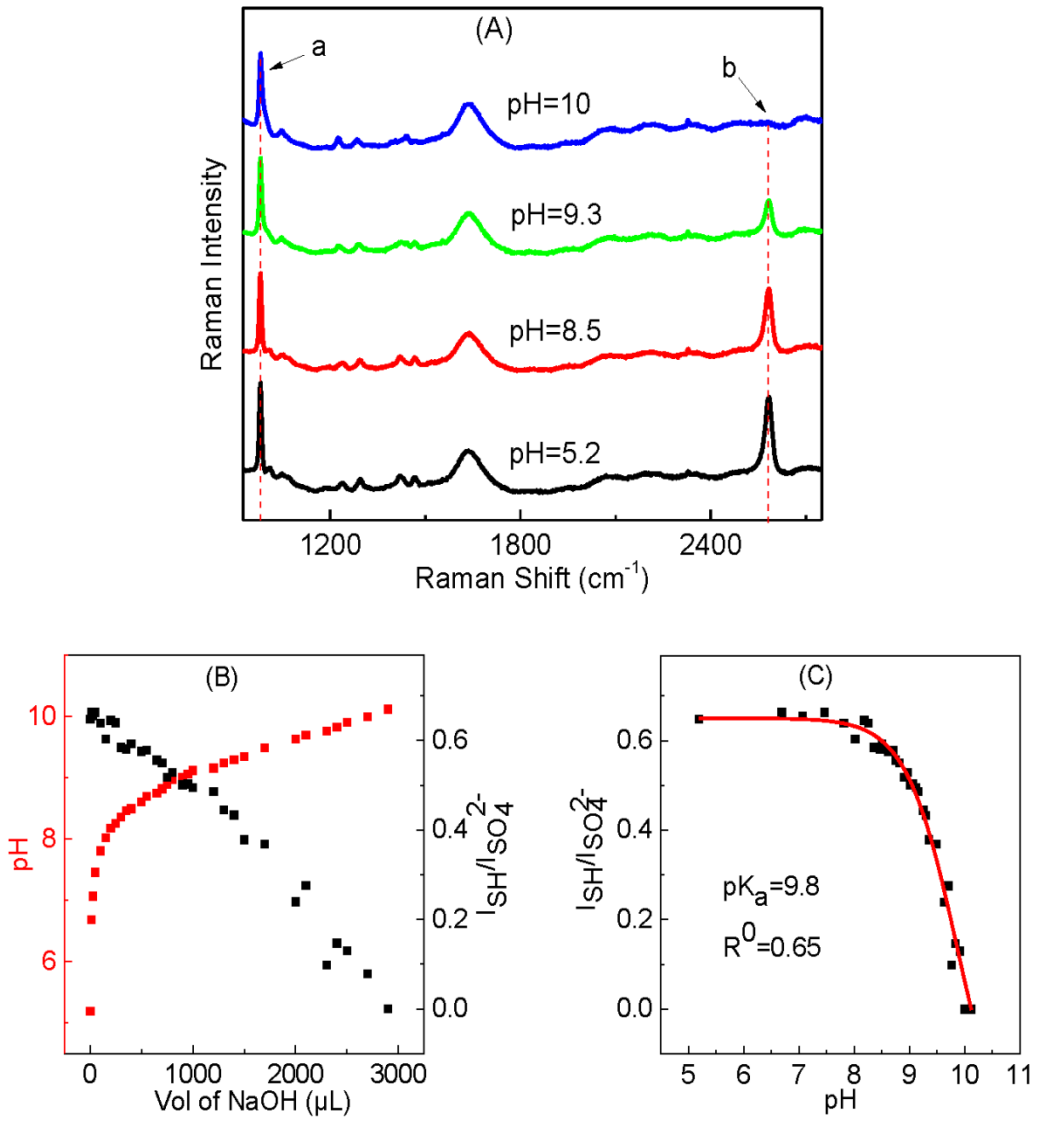

Figure 3.4 Raman-based pH titration for pK_a determination of the thiol group in 2-ME.

(A) Representative Raman spectra of 2-ME as a function of solution pH. ((a) SO_4^{2-}, (b) S-H peak). The spectra are normalized by the sulfate peak intensity. (B) Solution pH (red) and relative S-H peak intensity (black) as a function of titrant (500 mM NaOH) volume. (C) The relative S-H peak intensity as a function of solution pH. The solid curve and the data shown in (C) are the Boltzmann function curve-fitting output of the experimental data using Origin Pro. The 2-ME and Na_2SO_4 concentrations in the initial solutions are 0.42 M and 0.15 M, respectively.

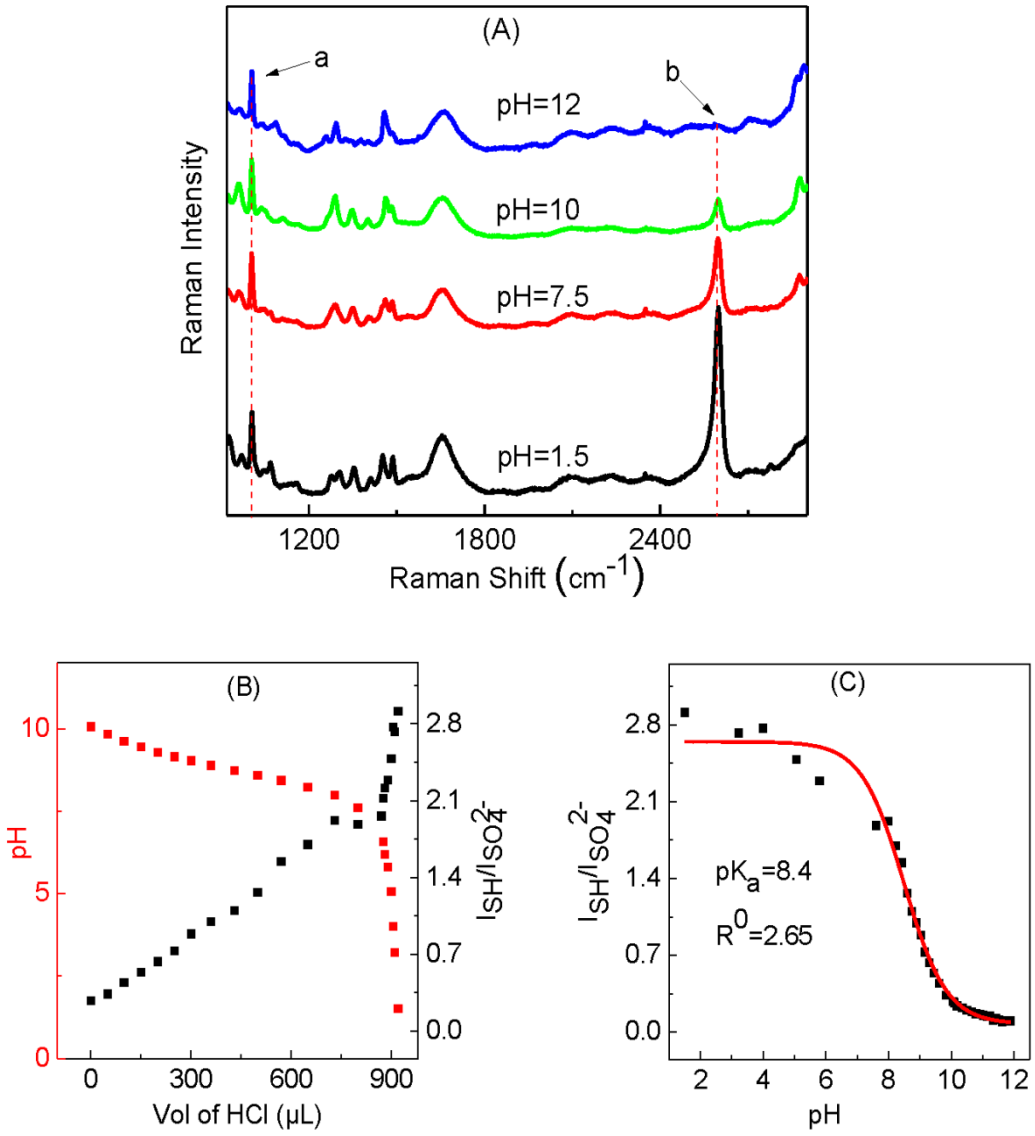

Figure 3.5 Raman-based pH titration for pK_a determination of the thiol group in CyA.

(A) Representative Raman spectra of CyA as a function of solution pH. ((a) SO_4^{2-}, (b) S-H peak). The spectra are normalized by the sulfate peak intensity. (B) Solution pH (red) and relative S-H peak intensity (black) as a function of titrant (1 M HCl) volume. (C) The relative S-H peak intensity as a function of solution pH. The solid curve and the data shown in (C) are the Boltzmann function curve-fitting output of the experimental data using Origin Pro. The CyA and Na_2SO_4 concentrations in the initial solutions are 2.5 M and 0.15 M, respectively.

As CyA forms a basic solution (pH ~11) once dissolved in water, it was titrated with 1 M HCl instead of NaOH to determine its pK_a.

The thiol pK_a values obtained with 3-MPS using three different internal reference peaks are highly similar (9.9 ±0.04). These internal references include a 980 cm^{-1} SO_4^{2-} peak from the exogenous Na_2SO_4, the C-H stretching feature (2930 cm^{-1}) and sulfonate (RSO_3^-, 1040 cm^{-1}) from 3-MPS itself. The fact that almost identical thiol pK_a values are obtained with the different reference peaks indicates the robustness of this internal-reference Raman titration technique.

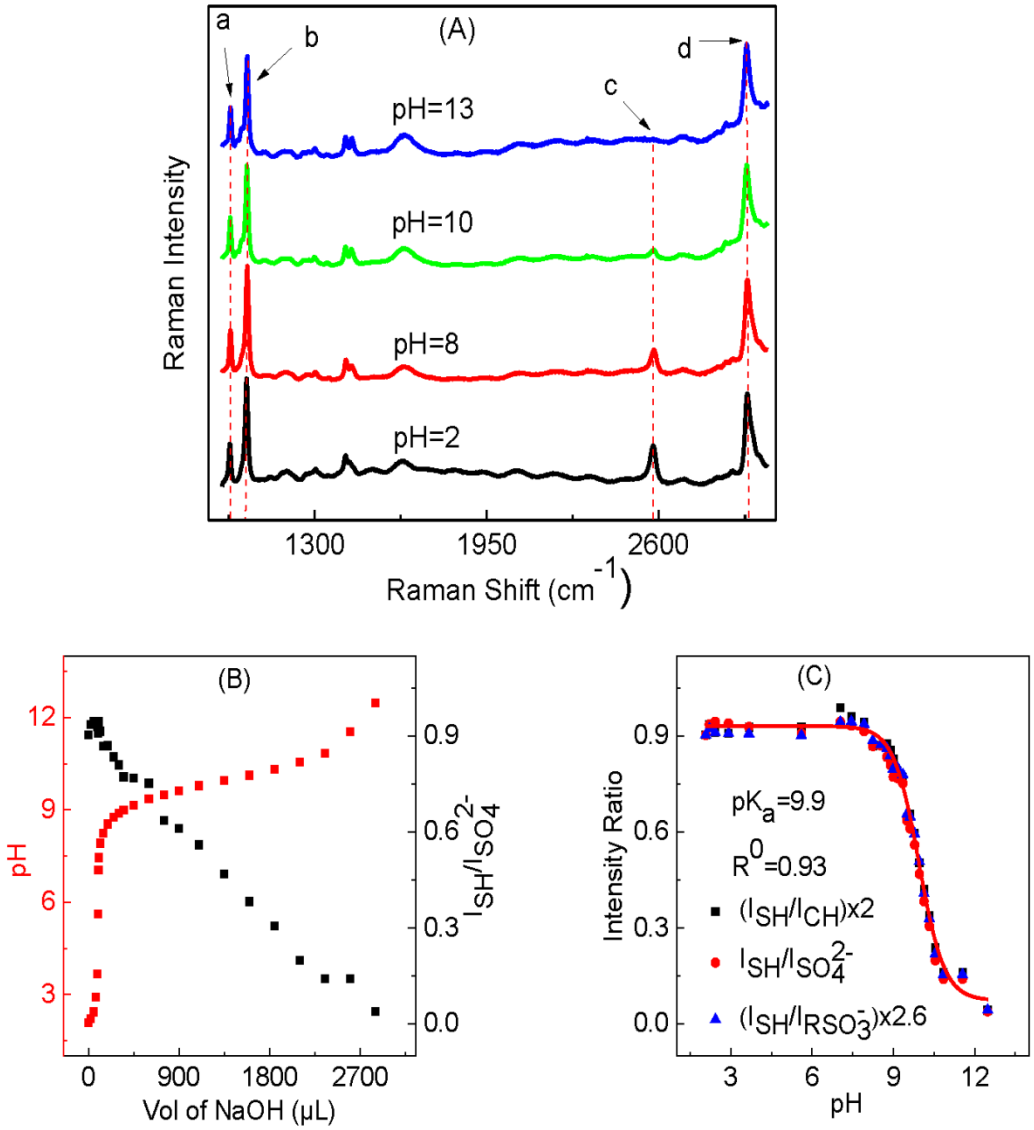

Figure 3.6 Raman-based pH titration for pK_a determination of the thiol group in 3-MPS.

(A) Representative Raman spectra of 3-MPS as a function of solution pH. The spectra are normalized by the sulfate peak intensity. The dotted line indicates the peak positions associated with the specified functional group. ((a) SO_4^{2-}, (b) RSO_3^-, (c) S-H, and (d) C-H peak). (B) Solution pH (red) and relative S-H peak intensity (black) as a function of titrant (500 mM NaOH) volume. (C) Intensity ratio of S-H stretching feature versus its internal reference peaks as a function of solution pH. The shapes in black, red and blue correspond to peak intensity ratio of S-H stretch versus its internal reference peak of the C-H, sulfate and sulfonate, respectively. The solid curve and the data shown in (C) are the Boltzmann function curve-fitting output of the experimental data using Origin Pro. The 3-MPS and Na_2SO_4 concentrations in the initial solutions are 0.68 M and 0.15 M, respectively.

It is also important to note that the pK_a values obtained with the peak intensity ratio are identical to that obtained with curve-fitting the integrated peak intensity ratios. Since the thiol pK_a values were determined by least-square fitting with this Raman titration data, the effect of random errors in the individual peak intensity ratios on the thiol pK_a values is insignificant.

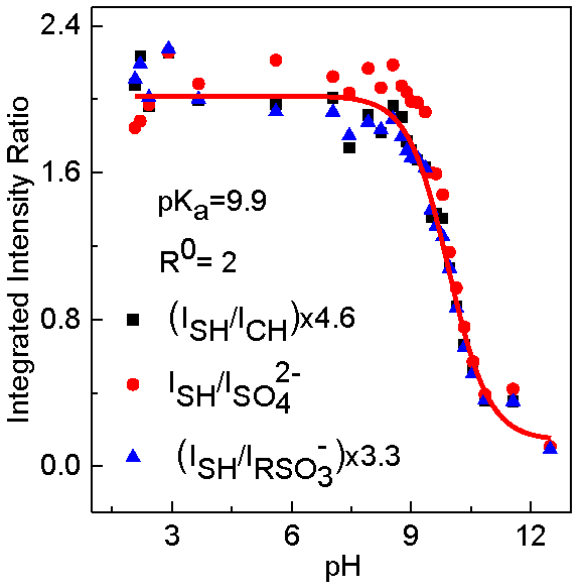

Figure 3.7 Integrated intensity ratio of S-H stretching feature versus its internal reference peaks for 3-MPS as a function of solution pH.

The shapes in black, red and blue correspond to the integrated intensity ratio of the S-H stretch versus the internal reference peak of C-H, sulfate and sulfonate, respectively. The solid curve and the data shown are the Boltzmann function curve-fitting output of the experimental data using Origin Pro. The 3-MPS and Na_2SO_4 concentrations in the initial solutions are 0.68 M and 0.15 M, respectively.

Table 3.1 summarizes the monothiol pK_a values explored in this work. Here the pK_a values determined with this method are very similar to the literature reported values. It indicates the applicability of this method for thiol pK_a determination.

Table 3.1 Monothiol pK_a values

Thiols	pK_a	
	This work	Literature value
Cys	8.6±0.04	8.3± 0.2[35]
GSH	9.2±0.3	9.2 ± 0.15[36]
2-ME	9.8±0.2	9.7[37]
CyA	8.4±0.05	8.35[38]
3-MPS	9.9±0.04	NA

3.5 Thiol pK_a of dithiols

The model dithiols (Figure 3.8) used in this work include DTT, 1,4-BDT, and 1,2-BDT.

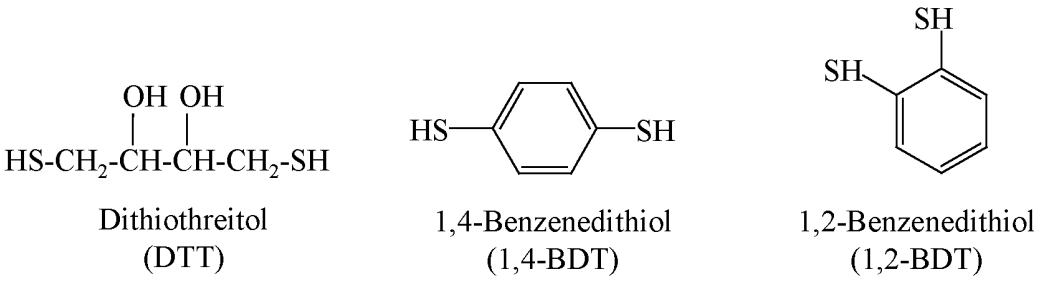

Dithiothreitol (DTT) | 1,4-Benzenedithiol (1,4-BDT) | 1,2-Benzenedithiol (1,2-BDT)

Figure 3.8 Structures of the model dithiols.

The Raman titration determination of the thiol pK_a values of water-soluble dithiol was demonstrated with DTT as the model dithiol. The first and second DTT thiol pK_a values, R^0, and α are 8.9, 10.3, 1.83, and 0.49, respectively. Their values were obtained by least squares curve-fitting the Raman titration data in Figure 3.9 (C) with Eq. 1.20 using the R program developed in this work. The pK_a values are in excellent agreement

with the literature reported DTT thiol pK_a values (9.2, and 10.1 for pK_{a1} and pK_{a2}, respectively).[39]

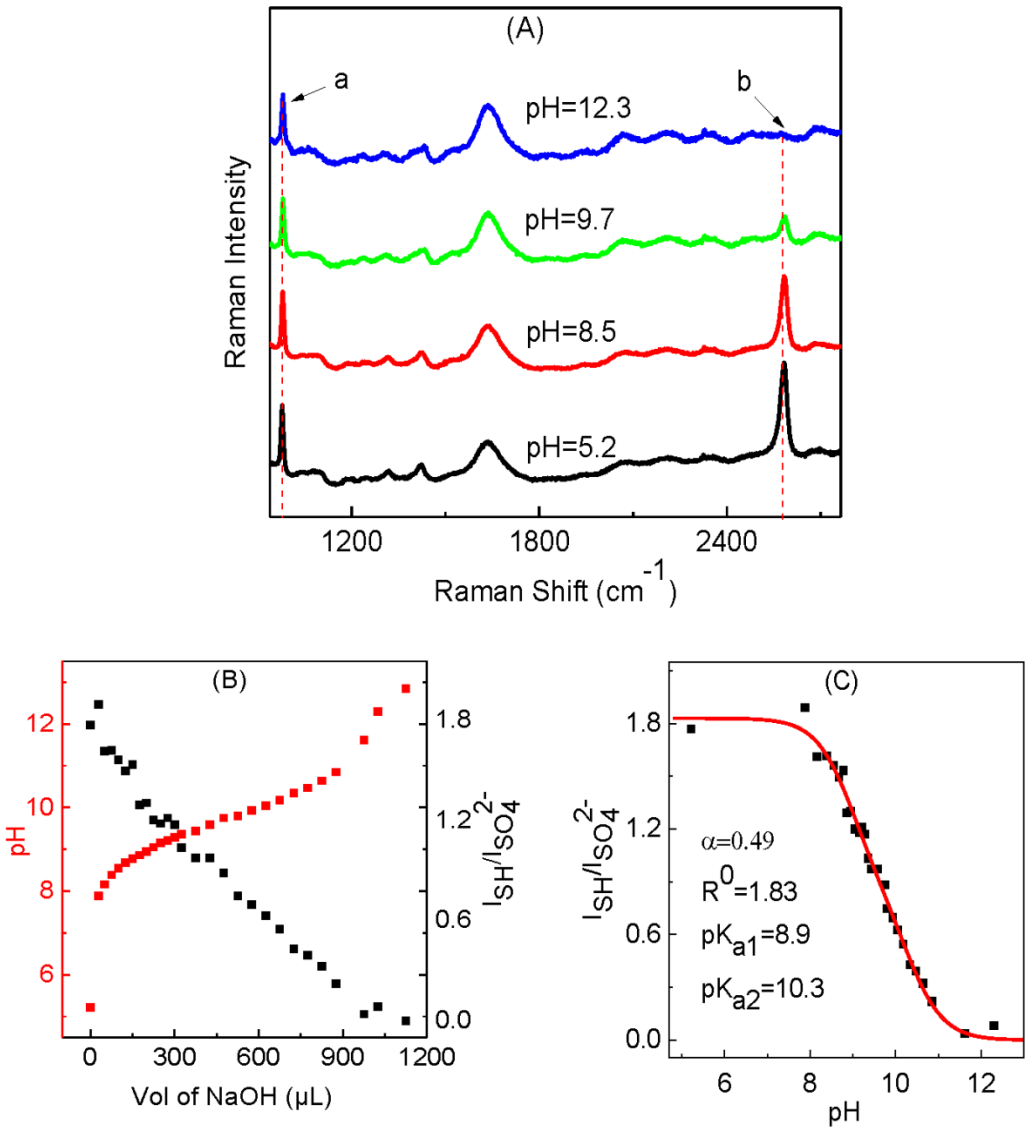

Figure 3.9 Raman-based pH titration for pK_a determination of the thiol groups in DTT.

(A) Representative Raman spectra of DTT as a function of solution pH. ((a) SO_4^{2-}, (b) S-H peak) The spectra are normalized by the sulfate peak intensity. (B) Solution pH (red) and relative S-H peak intensity (black) as a function of titrant (500 mM NaOH) volume. (C) The relative S-H peak intensity as a function of solution pH. The solid curve is by least-squares curve-fitting the experimental data with Eq. 1.20 using the R program. The pK_a values, R^0, and α are the curve-fitting outputs. The DTT and Na_2SO_4 concentrations in the initial titration solution are 0.65 M and 0.15 M, respectively.

The operational procedure of this internally-referenced Raman method is very straightforward for water-soluble thiols. However, many organothiols have low water solubility in their non-ionized form. Direct Raman titration of non-ionized thiols in water with NaOH can be difficult because the initial amount of thiol dissolved in solution is limited. In this case, it can be advantageous to use a reverse titration strategy in which the thiol is first dissolved in NaOH solution followed with HCl titration. This is because thiolates have higher solubility in water than non-ionized thiols.

The pK_a values of 1,4- and 1,2-BDT were explored with this reverse titration strategy (Figure 3.10 and 3.11) in which both BDT isomers were first dissolved in 1 M NaOH followed with HCl titration. Figure 3.10 (A) and 3.11 (A) show the representative Raman spectra for 1, 4- and 1, 2-BDT, respectively, both as a function of solution pH. The fact that there is a relatively intense and constant S-H feature in the 1,4-BDT solution when its pH changed from 10 to 13.6 indicates only one 1,4-BDT thiol is deprotonated even when the solution pH is as high as ~14. This result argues against the belief that the two 1,4-BDT thiols have similar pK_a values (pK_{a1}=6, pK_{a2}=7.7),[33] but it is consistent with a recent work conducted with a series of para-aryl dithiols (PADT) (HS-$(C_6H_5)_n$-SH, n=1, 2, and 3). This work showed that only one PADT thiol can be ionized even when PADT is reacted with molten NaOH at elevated temperature.[32] The fact that 1,4-BDT remains almost exclusively as monothiolate in the pH~13.6 solution indicates that the pK_a for the second 1,4-BDT thiol must be significantly higher than 14 in water.

Both non-ionized and monothiolated 1,4-BDT appear in the pH ~8.2 solution, indicating the first pK_a is close to pH value. However, Raman determination of the first pK_a value for 1,4-BDT thiol is not possible because of the following reasons. Obtaining

Raman spectra for 1,4-BDT at a solution pH lower than 8 is difficult since 1,4-BDT solubility at neutral and acidic pH is too low. The titration solutions at these pHs become very cloudy, making reliable Raman acquisition impossible.

The S-H stretching peak in the non-ionized and the monothiolated 1,4-BDT are at 2560 and 2480, respectively, differ by 80 cm^{-1} in which the vibrational frequency of S-H stretching in the monothiolated 1,4-BDT is significantly lower than that in its non-ionized counterpart. This large difference indicates that deprotonation of one thiol in the non-ionized 1,4-BDT has significant impact on the Raman feature of the remaining S-H bond. This red-shift of the S-H feature in the monothiolated 1,4-BDT is consistent with a previously proposed hypothesis that the remaining S-H in monothiolated 1,4-BDT is an effective hydrogen bond accepter, and the latter is responsible for the excellent dispersion stability of AuNPs functionalized with 1,4-BDT.[32] This conclusion is also consistent with the observation that hydrogen bonding induces a red-shift of the O-H stretch in water.[40-41]

The two thiols in 1,2-BDT are both deprotonated in the 1 M NaOH solution (Figure 3.11(C)). The first and second thiol pK_a values for 1,2-BDT are 6.5 and 10.9, respectively. This is in sharp contrast to 1,4-BDT for which only the first thiol can be ionized in water with a pK_a <8.2. Indeed, the first thiol pK_a value of 1,4-BDT must be higher than that for 1,2-BDT. Otherwise, no significant non-ionized 1,4-BDT Raman feature should appear in the Raman spectrum obtained with the pH ~8.2 solution. This degree of difference between the 1,2- and 1,4-BDT in their thiol pK_a values highlights the drastic isomerization effect on this aromatic molecule. The pK_a values for 1,2-BDT in water have, to our knowledge not been reported before. Only one 1,2-BDT thiol pK_a value (6.8) was reported and that is for 1,2-BDT dissolved in dimethyl sulfoxide.[42] It is

unclear whether this literature thiol pK_a refers to the average thiol pK_a for the two BDT thiols or for the first thiol.

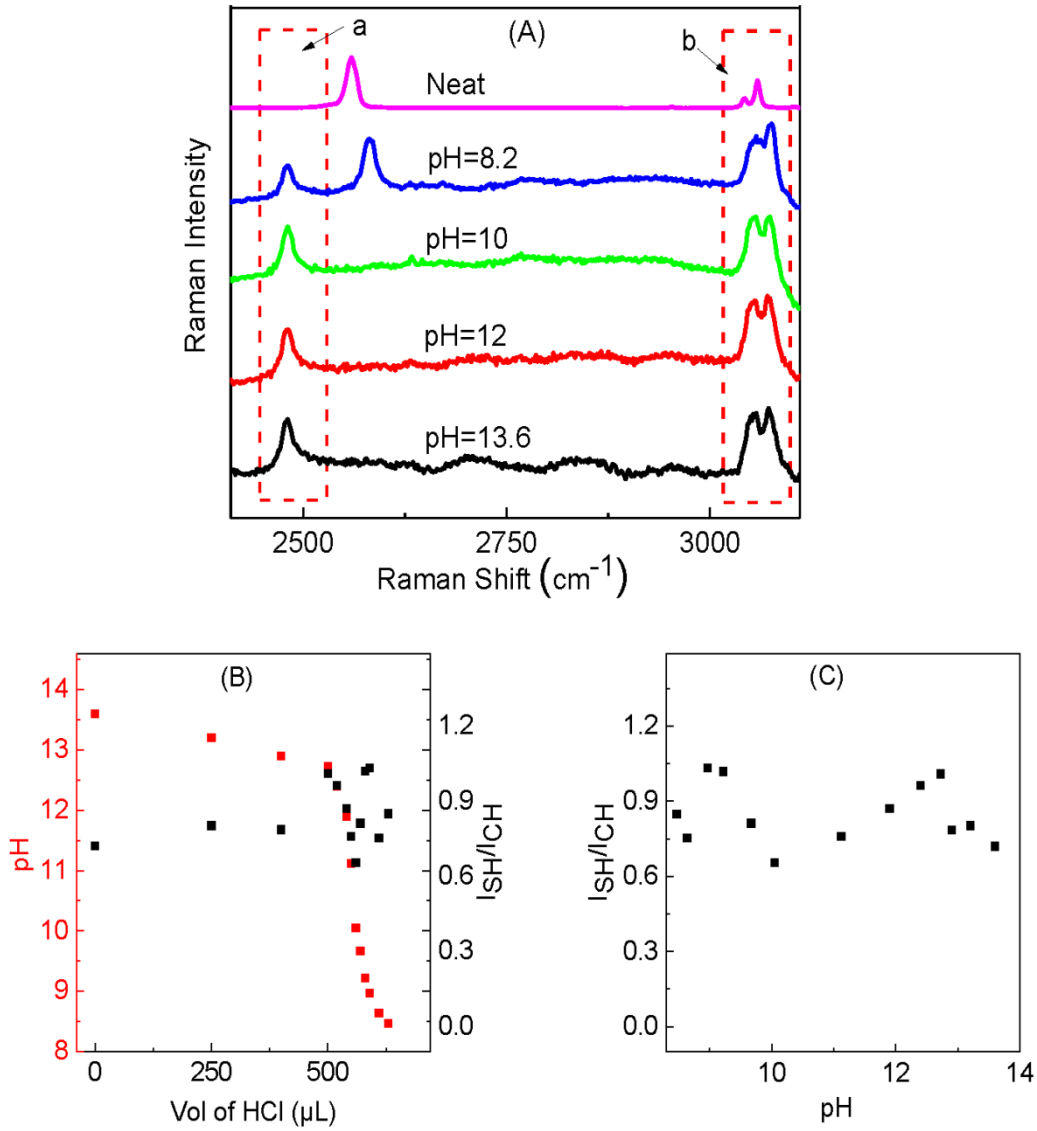

Figure 3.10 Raman-based pH titration for pK_a determination of the thiol groups in 1,4-BDT.

(A) Representative Raman spectra of 1,4-BDT as a function of solution pH. ((a) S-H, (b) C-H peak) The spectra are normalized by the C-H peak intensity. (B) Solution pH (red) and $I_{S\text{-}H}/I_{C\text{-}H}$ (black) as a function of titrant (1 M HCl) volume. (C) The relative S-H peak intensity as a function of solution pH.

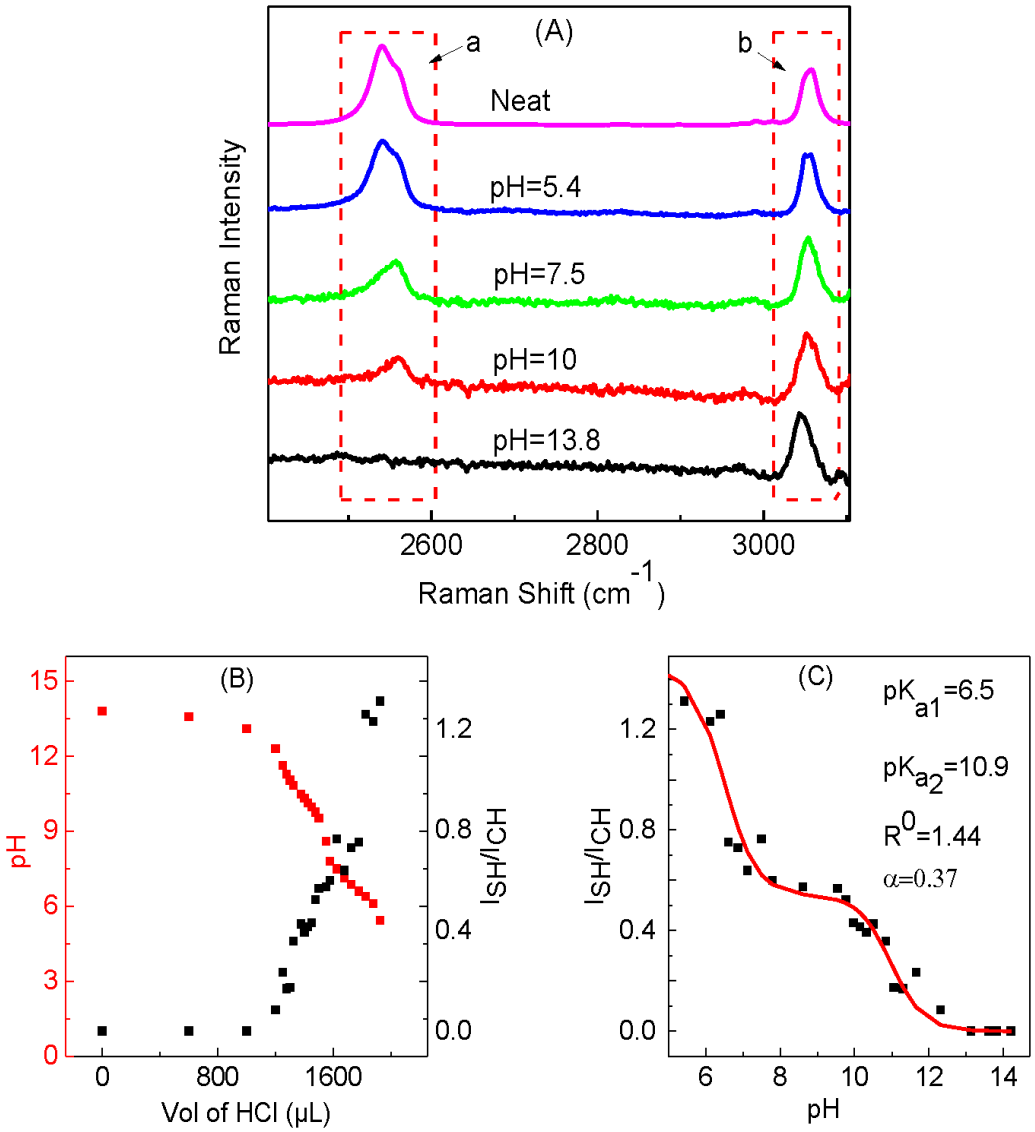

Figure 3.11 Raman-based pH titration for pK_a determination of the thiol groups in 1,2-BDT.

(A) Representative Raman spectra of 1,2-BDT as a function of solution pH. ((a) S-H, (b) C-H peak) The spectra are normalized by the C-H peak intensity. (B) Solution pH (red) and $I_{S\text{-}H}/I_{C\text{-}H}$ (black) as a function of titrant (1 M HCl) volume. (C) The relative S-H peak intensity as a function of solution pH. The solid curve is by least-squares curve-fitting the experimental data with Eq. 1.20 using the R program. The pK_a values, R^0, and α are the curve-fitting outputs.

The least-square curve-fitting method is very effective in pinpointing the correct pK_a values. Large error occurs even when only one of the two thiol pK_a values deviates

from the least-square value by as small as 0.5 pK_a (Figure 3.12). This further facilitates the fact that derived equation 1.20 can be readily used for the determination of dithiol pK_a values very accurately, using least-square curve-fitting.

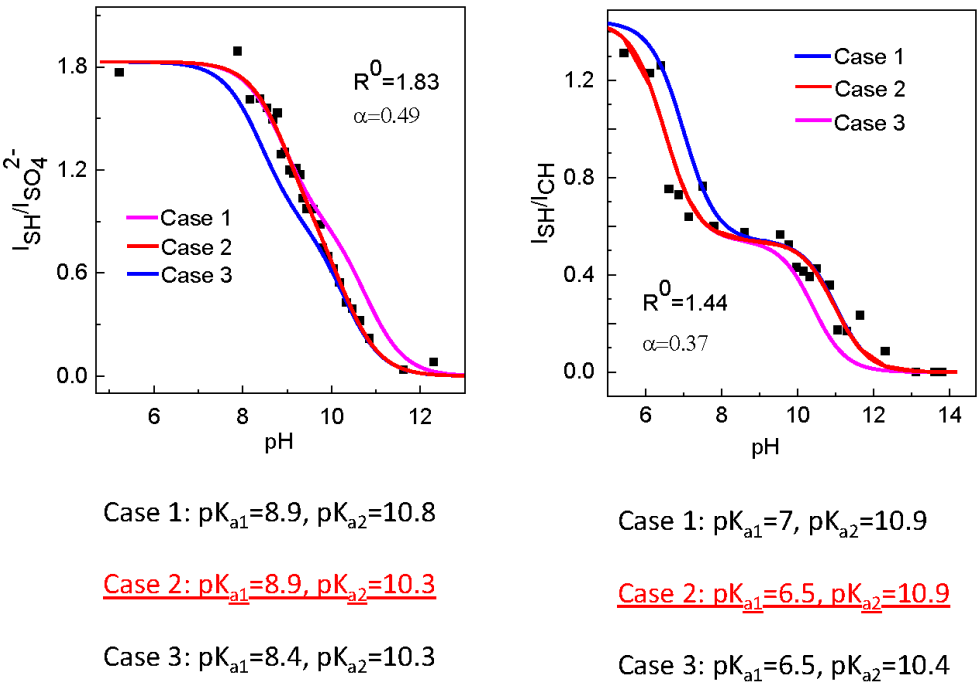

Case 1: pK_{a1}=8.9, pK_{a2}=10.8

Case 2: pK_{a1}=8.9, pK_{a2}=10.3

Case 3: pK_{a1}=8.4, pK_{a2}=10.3

Case 1: pK_{a1}=7, pK_{a2}=10.9

Case 2: pK_{a1}=6.5, pK_{a2}=10.9

Case 3: pK_{a1}=6.5, pK_{a2}=10.4

Figure 3.12 The relative S-H peak intensity as a function of solution pH of (A) DTT and (B) 1,2-BDT for three cases with different pK_{a1} and pK_{a2} values.

The solid curves are by least-squares curve-fitting the experimental data with Eq. 1.20. The pK_a values, R^0, and α are shown.

Table 3.2 Dithiol pK_a values.

Thiols	**Thiol pK_a**	
	This work	Literature value
DTT	8.9 (pK_{a1}) 10.3 (pK_{a2})	9.2 (pK_{a1})[39] 10.1(pK_{a2})[39]
1,4-BDT	< 8.2 (pK_{a1}) >14 (pK_{a2})	6 (pK_{a1})[33] 7.7 (pK_{a2})[33]
1,2-BDT	6.5 (pK_{a1}) 10.9 (pK_{a2})	6.8 in DMSO[42]

The pK_a values of the water-soluble dithiol, DTT, determined with this method is very similar to the literature reported values. However, there is a large difference in the thiol pK_a values determined in this work versus those reported for both of the two BDT isomers. This highlights the challenges in reliable thiol pK_a determination. Fruitfully, the Raman based method allows direct visualization of the degree of thiol ionization on the basis of the characteristic S-H feature. Therefore, it provides a simple means for one to evaluate the reliability of the literature thiol pK_a values.

3.6 Thiol Raman activity

Table 3.3 Thiol Raman activity

Thiols	**Relative thiol Raman activity ($\sigma_{SH}/\sigma_{SO_4^{2-}}$)**
Cys	0.22
GSH	0.23
2-ME	0.23
CyA	0.16
3-MPS	0.21
DTT	0.42 (for non-ionized DTT), 0.21 for monothiolated DTT
1,4-BDT	NA
1,2-BDT	NA

Table 3.3 summarizes the relative Raman activity for the mono- and di-thiols explored in this work. The relative Raman activities are represented by the Raman cross-section ratio of the thiol peak versus the SO_4^{2-} peak at 980 cm^{-1}. The thiol Raman activity in 1,2-and 1,4-BDT are not available because of the difficulty in determining the two BDT concentrations in their respective titration solution

Except for the thiol in CyA, all the thiols in the water-soluble thiols have similar Raman activities in which their relative Raman cross-section ratio of thiol versus SO_4^{2-} is ~0.22. This result is not surprising because the thiol groups are all directly linked to a saturated carbon. The reason that the CyA thiol has the lowest pK_a value and relative Raman activity among the tested water-soluble thiols is likely due to the presence of a positively charged primary amine group in CyA. The intramolecular electrostatic interaction facilitates the S-H ionization that explains the lower CyA thiol pK_a in comparison to the other thiols. This electrostatic interaction should also reduce the electron density surrounding the S-H group, leading to a reduced polarizability of this functional group and its lower Raman activity.

3.7 Conclusions

In summary, this work presents both the theoretical background and the experimental procedure including data analysis for Raman titration determination of the thiol pK_a values of both mono- and di-thiols in aqueous solutions. The application of this technique for water-soluble thiols is straightforward by direct titration of the thiols dissolved in water using NaOH. pK_a determination of poorly water soluble organothiols can be conducted by first dissolving the organothiols in NaOH followed with HCl titration. This internally-referenced Raman titration method is simple to implement and

its underlying theory is easy to follow. It should have broad applications for thiol pK_a determination and verification of literature thiol pK_a values.

REFERENCES

1. Skoog, D. A., West, D. M., Holler, F. J., Crouch, S. R.:*Fundamentals of Analytical Chemistry*; 9th ed.; Cengage Learning, 2013.

2. Nelson, D. A., Michael, M. C.: *Lehninger Principles of Biochemistry*; 6th ed.;W. H Freeman, New York, 2013.

3. Hupe, D.; Jencks, W.: *J.* Am*. Chem. Soc.* **1977**, *99*, 451-464.

4. Kreevoy, M. M.; Harper, E. T.; Duvall, R. E.; Wilgus III, H. S.; Ditsch, L. T.: *J. Am. Chem. Soc.* **1960**, *82*, 4899-4902.

5. Um, I. H.; Hong, Y. J.; Kwon, D. S.: *Tetrahedron* **1997**, *53*, 5073-5082.

6. Irving, R. J.; Nelander, L.; Wadso, J.: *Acta Chem. Scand.* **1964**, *18*, 769-787.

7. Harnsberger, H. F.; Cochran, E. L.; Szmant, H. H.: *J. Am. Chem. Soc.* **1955**, *77*, 5048-5050.

8. Vangala, K.; Ameer, F.; Salomon, G.; Le, V.; Lewis, E.; Yu, L.; Liu, D.; Zhang, D.: *J. Phys. Chem. C* **2012**, *116*, 3645-3652.

9. Lee, K. J.; Nallathamby, P. D.; Browning, L. M.; Osgood, C. J.; Xu, X.-H. N.:*ACS Nano* **2007**, *1*, 133-143.

10. Nie, Z.; Petukhova, A.; Kumacheva, E.: *Nat. Nanotechnol.* **2010**, *5*, 15-25.

11. Graham, D.; Thompson, D. G.; Smith, W. E.; Faulds, K.: *Nat. Nanotechnol.* **2008**,*3*, 548-551.

12. Erathodiyil, N.; Ying, J. Y.: *Acc. Chem. Res.* **2011**, *44*, 925-935.

13. Orendorff, C. J.; Gole, A.; Sau, T. K.; Murphy, C. J.: *Anal. Chem.* **2005**, *77*, 3261-3266.

14. Jozefczak, M.; Remans, T.; Vangronsveld, J.; Cuypers, A.: *Int. J. Mol. Sci.* **2012**,*13*, 3145-3175.

15. Seth, C.; Remans, T.; Keunen, E.; Jozefczak, M.; Gielen, H.; Opdenakker, K.; Weyens, N.; Vangronsveld, J.; Cuypers, A.: *Plant Cell Environ.* **2012**, *35*, 334-346.

16. Piste, P.: *Int. J. Pharm. Chem. Bio. Sci.* **2013**, *3*, 143-149.

17. Paulsen, C. E.; Carroll, K. S.: Chem. *Rev.* **2013**, *113*, 4633-4679.

18. Reijenga, J.; van Hoof, A.; van Loon, A.; Teunissen, B.: Anal. *Chem. Insights* **2013**, *8*, 53.

19. Mössner, E.; Iwai, H.; Glockshuber, R.: *FEBS Lett* **2000**, *477*, 21-26

20. DeCollo, T. V.; Lees, W. J.: *J. Org.* Chem. **2001**, *66*, 4244-4249.

21. Tajc, S. G.; Tolbert, B. S.; Basavappa, R.; Miller, B. L.: *J. Am. Chem. Soc.* **2004**,*126*, 10508-10509.

22. Danehy, J. P.; Parameswaran, K.: *J.* Chem. *Eng. Data* **1968**, *13*, 386-389.

23. Kortemme, T.; Creighton, T. E.: *J. Mol. Biol.* **1995**, *253*, 799-812.

24. Madzelan, P.; Labunska, T.; Wilson, M. A.: *FEBS J.* **2012**, *279*, 4111-4120.

25. Chivers, P. T.; Prehoda, K. E.; Volkman, B. F.; Kim, B.-M.; Markley, J. L.; Raines, R. T.: *Biochem.* **1997**, *36*, 14985-14991.

26. Colthup, N., Daly, L. H., Wiberley, S. E.: *Introduction to Infrared and Raman Spectroscopy*; 3rd ed.; Academic Press INC: New York, 1964.

27. Skoog, D. A., Holler, F. J., Crouch S. R.: *Principles of Instrumental Analysis*; 6th ed.; Cengage Learning, 2006.

28. Jeffery, G. H., Bassett, J., Mendham, J., Denney, R. C.: *Vogel's textbook of quantitative chemical analysis*; 5th ed.; John Wiley and Sons Inc, New York, 1989.

29. Ameer, F. S.; Zhou, Y.; Zou, S.; Zhang, D.: *J. Phys. Chem. C* **2014**, *118*, 22234-22242.

30. Langsetmo, K.; Fuchs, J. A.; Woodward, C.; Sharp, K. A.: *Biochem.* **1991**, *30*, 7609-7614.

31. Witt, A. C.; Lakshminarasimhan, M.; Remington, B. C.; Hasim, S.; Pozharski, E.; Wilson, M. A.: *Biochem.* **2008**, *47*, 7430-7440.

32. Gadogbe, M.; Chen, M.; Zhao, X.; Saebo, S.; Beard, D. J.; Zhang, D.: *J. Phys. Chem. C* **2015**, *119*, 6626-6633.

33. Armstrong, D. A.; Sun, Q.; Tripathi, G. N. R.; Schuler, R. H.; McKinnon, D.: *J. Phys. Chem.* **1993**, *97*, 5611-5617.

34. Li, H.; Hanson, C.; Fuchs, J. A.; Woodward, C.; Thomas, G. J.: *Biochemistry* **1993**, *32*, 5800-5808.

35. Krekel, F.; Samland, A. K.; Macheroux, P.; Amrhein, N.; Evans, J. N. S.: *Biochemistry* **2000**, *39*, 12671-12677.

36. Tang, S.-S.; Chang, G.-G.: *J. Biochem*. **1996**, *119*, 1182-1188.

37. Jencks, W. P.; Salvesen, K.: *J. Am.* Chem. *Soc.* **1971**, *93*, 4433-4436.

38. Connett, P.; Wetterhahn, K.: *J. Am.* Chem. *Soc.* **1986**, *108*, 1842-1847.

39. Szajewski, R. P.; Whitesides, G. M.: *J. Am. Chem. Soc.* **1980**, *102*, 2011-2026.

40. Auer, B.; Kumar, R.; Schmidt, J.; Skinner, J.: *Proc Natl Acad Sci* **2007**, *104*, 14215-14220.

41. Liu, Y.; Ojamäe, L.: *J. Mol.* Model. **2014**, *20*, 1-8.

42. Yu, H.-Z.; Yang, Y.-M.; Zhang, L.; Dang, Z.-M.; Hu, G.-H.: *J. Phys. Chem. C* **2014**, *118*, 606-622.

APPENDIX A

R CODE

A.1 R code for least square curve-fitting with Eq. 1.20

```
####fr is the least square function that need to be optimized####
fr=function(par,ph,Rph){
 R0=par[1]
alpha=par[2]
pka1=par[3]
pka2=par[4]
sum(((R0+alpha*R0*10^(ph-pka1))/(1+10^(ph-pka1)*(1+10^(ph-pka2)))-Rph)^2)
}
##############################################################################
#
##############
# pka.fit is the function to fit the parameters
#
# par is a vector of the initial guess for the parameters R0,alpha, pka1 and pka2
#
# ph is the experimental value for ph
#
# Rph is the experimental value for Rph
#
# Returning values are fitted parameters, fitted Rph and MSE
#
##############################################################################
#
##############

pka.fit=function(par,ph,Rph){
res=optim(par, fr, ph=ph,
Rph=Rph)
R0.f=res$par[1]
alpha.f=res$par[2]
pka1.f=res$pa[3]
pka2.f=res$par[4]
Rph.f=(R0.f+alpha.f*R0.f*10^(ph-pka1.f))/(1+10^(ph-pka1.f)*(1+10^(ph- pka2.f)))
MSE=sum((Rph.f-Rph)^2)
return(list(R0.f=R0.f,alpha.f=alpha.f,pka1.f=pka1.f,pka2.f=pka2.f,Rph.f=Rph.f,
MSE=MSE))}
```